

# Electroacoustic Phenomena in Concentrated Dispersions: New Theory and CVI Experiment

A. S. Dukhin,<sup>\*,†</sup> V. N. Shilov,<sup>‡</sup> H. Ohshima,<sup>§</sup> and P. J. Goetz<sup>†</sup>

Dispersion Technology Inc., 3 Hillside Avenue, Mount Kisco, New York 10549,  
Faculty of Pharmaceutical Sciences and Institute of Colloid and Interface Science,  
Science University of Tokyo, 12 Ichigaya Funagawara-machi, Shinjuku-ku, Tokyo 162-0826,  
Japan, and Institute of Biocolloid Chemistry, Academy of Sciences of the Ukraine,  
Kiev, Ukraine

Received March 16, 1999. In Final Form: June 2, 1999

There are two quite different approaches to deriving an electroacoustic theory. The first was suggested by Enderby and Booth 50 years ago and later modified by Marlow, Fairhurst and Pendse. The second was suggested by O'Brien about 10 years ago (O'Brien's approach). He introduced a special relationship between kinetic coefficients that is assumed to be valid in a concentrated system. This approach requires also a theory for dynamic electrophoretic mobility. The most recent version of this theory for concentrated systems was created by Ohshima, Shilov, and A. Dukhin on the basis of the cell model. A hybrid of the O'Brien relationship and this new electrophoretic mobility theory yields expressions for electroacoustic effects in the concentrated systems. We call it "hybrid O'Brien's theory". In principle these two approaches must lead to the same result. To test this expectation, we should generalize the first approach such that it is valid for concentrates. We have done this using the Kuvabara cell model for calculating the hydrodynamic drag coefficient and the Shilov-Zharkikh cell model for electrokinetics. In addition we used a well-known "coupled phase model" for describing the relative motion between the particles and the liquid in the concentrated system. The coupled phase model allows us to eliminate superposition assumption for hydrodynamic fields for incorporating particle polydispersity into the theory. For dilute systems the new theory gives exactly same result as O'Brien's dilute case theory. Surprisingly, in the concentrated systems this theory yields a new relationship for electroacoustic phenomena. It does not converge to the "hybrid O'Brien theory". Why? It turned out that O'Brien's relationship contradicts the Onsager relationship in concentrated systems at the extreme case of the low frequencies when the Onsager relationship is valid. The new theory satisfies the Onsager principle and it converges to the Smoluchowski limit at any volume fraction assuming thin double layer and negligible surface conductivity. We have tested this new theory experimentally using silica Ludox TM (30 nm) and rutile R-746 Dupont (about 300 nm). In both cases we performed an equilibrium dilution protocol. This experimental test confirmed our new theory for volume fractions up to 45 vol %. It also showed that O'Brien's relationship leads to hundreds percents of error in concentrated systems. It is important to mention here the difference between the original O'Brien's theory and software used in the commercially available electroacoustic spectrometer Acoustosizer. This instrument employs O'Brien's method, but it contains an additional unavailable empirical correction (Hunter, R. J. *Colloids Surf.* **1998**, *141*, 37-65) for concentrates. This empirical correction masks original theoretical results.

## Introduction

There are two quite different approaches to deriving an electroacoustic theory. Historically the first began with works by Enderby and Booth.<sup>2,3</sup> They simply tried to solve a system of classical electrokinetic equations without using any thermodynamic relationships. It was very complex because they took into account surface conductivity effects. Although this initial theory was valid only for dilute systems, this approach was later expanded by Marlow, Fairhurst, and Pendse,<sup>4</sup> who tried to generalize it for concentrated systems using a Levine cell model.<sup>5</sup> This approach leads to somewhat complicated mathematical formulas. Perhaps this was the reason it was abandoned.

An alternative approach to electroacoustic theory was suggested later by O'Brien.<sup>6</sup> He introduced the concept of a dynamic electrophoretic mobility  $\mu_d$  and derived a relationship between this parameter and the measured electroacoustic parameters such as colloid vibration current (CVI) or electrosonic amplitude (ESA):

$$\text{ESA(CVI)} = C_{\text{cell}} \sigma q \mu_d E(\nabla P) \quad (1)$$

where  $C_{\text{cell}}$  is a cell constant,  $q$  is the volume fraction of solid,  $P$  is the hydrodynamic pressure, and  $E$  is the external electric field strength. The parameter  $\sigma$  is a contrast between particle density ( $\rho_p$ ) and liquid density ( $\rho_m$ ):

$$\sigma = \frac{\rho_p - \rho_m}{\rho_m} \quad (2)$$

Later O'Brien stated that his relationship is valid for concentrated systems as well.

According to O'Brien, a complete functional dependence of ESA(CVI) on key parameters such as  $\zeta$ -potential,

<sup>1</sup> Dispersion Technology Inc.

<sup>†</sup> Academy of Sciences of the Ukraine.

<sup>§</sup> Science University of Tokyo.

(1) Hunter, R. J. Recent developments in the electroacoustic characterization of colloidal suspensions and emulsions. *Colloids Surf.* **1998**, *141*, 37-65.

(2) Booth, F.; Enderby, J. On Electrical Effects due to Sound Waves in Colloidal Suspensions. *Proc. Am. Phys. Soc.* **1952**, *208A*, 32.

(3) Enderby, J. A. On Electrical Effects Due to Sound Waves in Colloidal Suspensions. *Proc. R. Soc., London* **1951**, *A207*, 329-342.

Both particles and liquid move with an acceleration created by the sound wave pressure gradient. In addition, because of inertia effects, the particles move relative to the liquid which causes viscous friction forces acting between the particles and liquid.

The balance of these forces can be presented using the following system of equations written separately for particles and liquid:

$$-q \nabla P = q \rho_p \frac{\partial u_p}{\partial t} + \gamma(u_p - u_m) \quad (3)$$

$$-(1 - q) \nabla P = (1 - q) \rho_m \frac{\partial u_m}{\partial t} - \gamma(u_p - u_m) \quad (4)$$

where  $u_m$  and  $u_p$  are velocities of the medium and particles in the laboratory frame of reference,  $t$  is time, and  $\gamma$  is a friction coefficient which is proportional to the volume fraction and particle hydrodynamic drag coefficient  $\Omega$ :

$$\gamma = \frac{9\eta q \Omega}{2a^2}$$

$$F_r = 6\pi\eta a \Omega (u_p - u_m)$$

where  $\eta$  is dynamic viscosity and  $a$  is the particle radius.

This system of equations (3) and (4) is well-known in the field of acoustics. It has been used in several papers<sup>13-16</sup> for calculating sound speed and acoustic attenuation. It is valid without any restriction on volume fraction. Importantly, it is known that this system of equations yields a correct transition to the dilute case.

This system of equations is normally referred to as the "coupled phase model". The word "model" usually suggests the existence of some alternative formulation, but it is hard to imagine what one can change in this set of force balance equations, which essentially express Newton's second law. Perhaps the word "model" is too pessimistic in this case.

This system of equations can be solved for the speed of the particle relative to the liquid. The time and space dependence of the unknown  $u_m$  and  $u_p$  is presented as a monochromatic wave  $Ae^{j(\omega t - l x)}$ , where  $j$  is a complex unit and  $l$  is a complex wavenumber. As a result, the system of equations (3) and (4) yields the following relationship between the gradient of pressure and the speed of the particle relative to the fluid:

$$\gamma(u_p - u_m) = \frac{q(\rho_p - \rho_s)}{\rho_s + i\omega q(1 - q)(\rho_p \rho_m / \gamma)} \nabla P \quad (5)$$

where  $\rho_s = q\rho_p + (1 - q)\rho_m$ ;  $q$  is volume fraction of the solid particles.

The relative motion of the particles ( $u_p - u_m$ ) disturbs the double layers surrounding the particles and consequently induces electroacoustic phenomena. This relationship between the particle motion and the resulting electroacoustic signal is described next.

**CVI as a Sedimentation Current.** Sedimentation current is well-known from classical colloid chemistry handbooks.<sup>12,17,18</sup> Simply put, charged particle sediment due to gravity will develop a sedimentation potential between two vertically spaced electrodes. If we externally short circuit these electrodes, the current which flows is referred to as sedimentation current. We can extend this simple concept to include colloid vibration current by simply replacing the acceleration of gravity with analogous

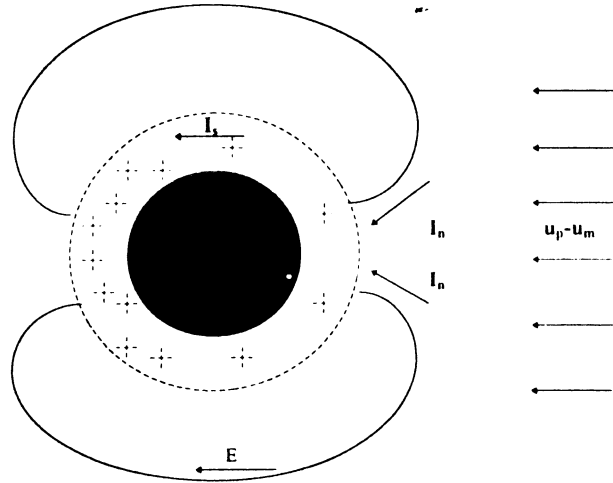


**Figure 2.** Mechanism of the double layer polarization generating sedimentation current for a single particle.

acceleration caused by the applied acoustic field. This idea is described in more detail in the last section.

Figure 2 illustrates a particle with a double layer moving relative to the liquid. This motion involves ions of the double layer. In this case we consider only the positive counterions opposing the negatively charged particle surface. The hydrodynamic surface current  $I_s$  reduces the number of positive ions near the right particle pole and enriches the double layer with extra ions near the left pole. As a result, the double layer shifts from the original equilibrium. The negative surface charge dominates at the right pole whereas extra positive diffuse charge dominates at the left pole. The net result is that the motion has induced a dipole moment.

This induced dipole moment generates an electric field which is usually referred to as a colloid vibration potential (CVP). This CVP is external to the particle double layer. It affects ions in the bulk of the electroneutral solution beyond the double-layer-generating electric current  $I_n$ . This electric current serves a very important purpose. It compensates for the surface current  $I_s$  and makes the whole picture self-consistent.

The next step is to add a quantitative description to this simple qualitative picture. To do this we must find a relationship between the CVP and  $u_p - u_m$ . Appendix 1 gives a complete mathematical description of this problem. We solved this problem using the Shilov-Zharkikh cell model.<sup>19</sup> Advantages of this cell model over the Levine cell model<sup>5</sup> are given in ref 9.

Calculations yield the following expression for colloid vibration current (CVI):

$$CVI = CVP * K_s = \frac{3\epsilon\epsilon_0\zeta K_s^{\text{cs}}}{K_m a} \frac{q}{1 - q} \frac{\partial u_\theta}{\sin \theta \partial r} \quad (6)$$

where  $\epsilon$  and  $\epsilon_0$  are the dielectric permittivities of the medium and vacuum,  $\zeta$  is the electrokinetic potential,  $a$  is the particle radius,  $K_m$  and  $K_s$  are complex conductivities of the medium and system,  $q$  is the volume fraction,  $r$  and  $\theta$  are the spherical coordinates associated with the particle center, and  $u_r$  and  $u_\theta$  are the radial and tangential velocities of the liquid motion relative to the particle.

The next step in the development of this CVI theory is the calculation of the hydrodynamic field assuming that the speed of particle with respect to the liquid is given by expression 5. This is done in the next section and Appendix 2.

**Calculation of Hydrodynamic Field Using the Nonstationary Kuvabara Cell Model.** In this section we calculate the particle drag coefficient  $\gamma$  and tangential speed of the liquid  $u_\theta$  which is a part of eq 6. We will perform this calculation assuming that liquid is incompressible. This condition is valid only when wavelength  $\lambda$  is much larger than particle size:

$$\lambda \gg a \quad (7)$$

This is the so-called long wavelength requirement. It allows us to use traditional hydrodynamic equations for liquid velocity  $u$  and hydrodynamic pressure  $P$ :

$$\rho_m \frac{du}{dt} = \eta \operatorname{rot} \operatorname{rot} u + \operatorname{grad} P \quad (8)$$

$$\operatorname{div} u = 0 \quad (9)$$

This system of equations has been solved by A. Dukhin et al.<sup>15</sup> for a Happel cell model. Here we suggest another solution using the Kuvabara cell model. Both models apply the same boundary conditions at the surface of the particle:

$$u_r(r=a) = u_p - u_m \quad (10)$$

$$u_\theta(r=a) = -(u_p - u_m) \quad (11)$$

However, the boundary conditions at the surface of the cell are quite different for the Kuvabara cell model and are given by the following equations:

$$\operatorname{rot} u_{r=b} = 0 \quad (12)$$

$$u_r(r=b) = 0 \quad (13)$$

The general solution for the velocity field contains three unknown constants  $C$ ,  $C_1$  and  $C_2$ :

$$u_r(r) = C \left( 1 - \frac{b^3}{r^3} \right) + 1.5 \int_r^b \left( 1 - \frac{x^3}{r^3} \right) h(x) dx \quad (14)$$

$$u_\theta(r) = -C \left( 1 + \frac{b^3}{2r^3} \right) - 1.5 \int_r^b \left( 1 + \frac{x^3}{2r^3} \right) h(x) dx \quad (15)$$

$$h(x) = C_1 h_1(x) + C_2 h_2(x) \quad (16)$$

The values of these constants and special functions are given in Appendix 2.

The final expressions for the drag coefficient and tangential velocity are

$$\gamma = \omega \rho_m \varphi \left[ \frac{3}{4I} \left( -\frac{dh}{dx} + \frac{h}{x} \right)_{x=a} - J \right] \quad (17)$$

$$\frac{du_\theta}{dr_{r=a}} = \frac{3(u_p - u_m)h(\alpha)}{2I} \quad (18)$$

where  $\alpha = a(\omega^{1/2}/2\nu)$ ,  $\beta = ba/a$ ,  $\nu$  is kinematic viscosity, and  $\eta$  is dynamic viscosity. The values of the special functions  $h(x)$  and  $I(x)$  are presented in Appendix 2.

**CVI for Monodisperse System.** Substituting the drag coefficient into eq 5 and applying the result to eq 6 give

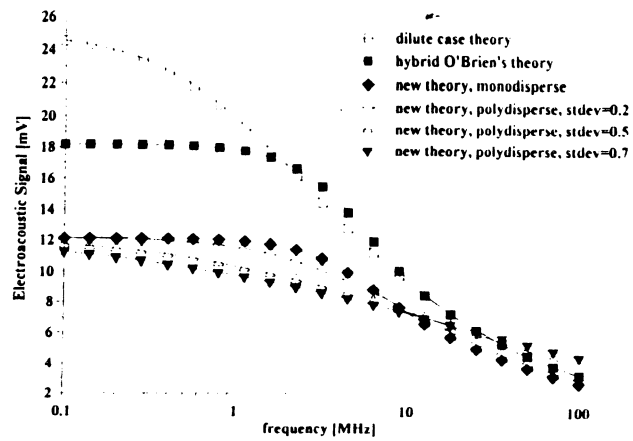


**Figure 3.** Theoretically calculated normalized CVI (eq 22) versus frequency for dispersion with 20 vol % of 1  $\mu\text{m}$  particles. Density of the liquid is 1  $\text{g}/\text{cm}^3$ , of the particles – 2  $\text{g}/\text{cm}^3$ .

us the following expression for CVI:

$$\text{CVI} = \frac{3\epsilon\epsilon_0\zeta(1-q)\varphi(\rho_p - \rho_s)}{2\eta(1+0.5q)} \frac{H + [I/(1-q)]}{1.5H - \frac{(1-q)\rho_p - \rho_s}{\rho_s} I} \nabla P \quad (19)$$

In deriving this equation we used the Maxwell–Vagner relationship between conductivity of the system and the conductivity of the medium:<sup>21</sup>

$$\frac{K_s}{K_m} = \frac{1-q}{1+0.5q} \quad (20)$$

This expression is valid for nonconducting particles, thin double layer, and for low surface conductivity ( $Du \ll 1$ ).

It is possible to show that eq 19 converges to O'Brien's dilute case theory when  $q \rightarrow 0$ .

At the same time this result for CVI differs significantly from the expression for CVI obtained on the basis of the same cell model for dynamic electrophoretic mobility and O'Brien's relationship in concentrated systems.<sup>10</sup> This theory which we referred to as "hybrid O'Brien's theory" yields the following expression for CVI:

$$\text{CVI}^\circ = \frac{3\epsilon\epsilon_0\zeta(1-q)\varphi(\rho_p - \rho_m)}{2\eta(1+0.5q)} \frac{H + [I(1-q)]}{1.5H - \frac{\rho_p - \rho_m}{\rho_m} I} \nabla P \quad (21)$$

Figure 3 illustrates the differences between two theories for dispersion with 20 vol % of 1  $\mu\text{m}$  particles. The density of the particles is 2  $\text{g}/\text{cm}^3$ , the density of the medium is 1  $\text{g}/\text{cm}^3$ , and the  $\zeta$ -potential is 25 mV. The electroacoustic signal is dimensioned according to the following expression:

$$\text{electroacousticSignal} = \text{CVI} \frac{2\eta\rho_m}{3\epsilon\epsilon_0\varphi(\rho_p - \rho_m)} \quad (22)$$

(20) Lyklema, J. *Fundamentals of Interface and Colloid Science*; Academic Press: New York, 1993; Vol. 1.

(21) Dukhin, S. S.; Shilov, V. N. *Dielectric Phenomena and the Double Layer in Disperse Systems and Polyelectrolytes*. John Wiley & Sons: New York, 1974.

**CVI for Polydisperse System.** Let us assume now that we have a polydisperse system with conventional  $N$  fractions. Each fraction of particles has certain particle diameter  $d_i$ , volume fraction  $\phi_i$ , drag coefficient  $\gamma_i$ , and particle velocity  $u_i$  in the laboratory frame of reference. We assume the density of the particles to be the same for all fractions  $\rho_p$ . The total volume fraction of the dispersed phase is  $\phi$ . The liquid is characterized by dynamic viscosity  $\eta$ , density  $\rho_m$ , and velocity in the laboratory frame of reference  $u_m$ .

The coupled phase model<sup>13-16</sup> allows us to calculate difference the  $u_i - u_m$  for each fraction without using the supersposition assumption. The coupled phase model suggests applying force balance to each fraction of the dispersed system including dispersion medium. We did it before for one fraction. Now we apply the same principle to the  $N$  fractions and obtain the following system of  $N + 1$  equations:

$$-\phi^i \Delta P = \phi^i d^i \rho^i \omega u_i + \gamma^i (u_i - u_m) \quad (23)$$

$N$  equation for particles

$$-\phi^i \Delta P = \phi^i d^i \rho^i \omega u_i + \gamma^i (u_i - u_m) - \phi^i \Delta P = (1 - \phi) \Delta P = (1 - \phi) \rho_m \omega u_m - \sum_{i=1}^N \gamma^i (u_i - u_m) \quad (24)$$

where  $j$  is a complex unit,  $P$  is pressure, and  $\omega$  frequency of the ultrasound,

$$\gamma_i = \frac{18 \eta \phi_i \Omega}{d_i^2}$$

$$F_{\text{Sokes}}^i = 3 \pi \eta d \Omega (u_i - u_m)$$

We can solve the system of  $N + 1$  equations following our previous paper.<sup>15</sup> To do this, we reformulate all equations introducing desirable quantities  $x_i = u_i - u_m$  and eliminate parameter  $u_m$  using the last equation which specifies the liquid velocity in the form

$$u_m = - \frac{\Delta P}{\sum_{i=1}^N \gamma^i x_i} + \frac{\sum_{i=1}^N \phi^i \rho^i \omega x_i (1 - \phi) \rho_m}{\Delta P} \quad (25)$$

The new system of  $N$  equations is

$$\left( \frac{\rho^i}{\rho^p} - 1 \right) \Delta P = \left( \frac{\phi^i}{\gamma^i} + \frac{\phi^i}{\rho^p} \right) x_i + \frac{\sum_{i=1}^N \phi^i \rho^i \omega x_i (1 - \phi) \rho_m}{\sum_{i=1}^N \gamma^i x_i} \quad (26)$$

This system can be solved using the principle of mathematical induction. We guess a solution for  $N$  fractions and then prove that the same solution works for  $N + 1$  fraction. As a result, we obtain the following expression for velocity of the  $i$ th fraction particle relative to the liquid:

$$u_i - u_m = \frac{\left( \frac{\rho^i}{\rho^p} - 1 \right) \Delta P}{\left( \frac{\phi^i}{\gamma^i} + \frac{\phi^i}{\rho^p} \right) + \frac{\sum_{i=1}^N \phi^i \rho^i \omega x_i (1 - \phi) \rho_m}{\sum_{i=1}^N \gamma^i x_i}} \quad (27)$$

This equation is the result of the first step of the electroacoustic theory for the polydisperse system. The next step is calculation of the corresponding electric field. We can do this using eq 1.14. We can apply the same equation for calculating the electric field generated by the  $i$ th fraction of the polydisperse system CVP, keeping in mind that number of dipoles in this fraction is  $q_i/y$  times less

$$\text{CVP}_i = \frac{3 \epsilon \epsilon_0 q_i^2}{a_i^2} \frac{K_m \phi^i}{b_i^3 - a_i^3} \frac{1}{\sin \theta} \frac{\partial r}{\partial r_a} \quad (28)$$

This equation has been derived using the cell model. Usually, the cell model is formulated for a monodisperse system. We offered in our previous paper<sup>15</sup> the way to generalize the cell model for polydispersity. Here we just repeat our old work. Each fraction can be characterized by particle radii  $a_i$ , cell radii  $b_i$ , thickness of the liquid shell in the spherical cell  $l_i = b_i - a_i$ , and volume fraction  $\phi_i$ . The mass conservation law relates these parameters together as follows:

$$\sum_{i=1}^N \left( 1 + \frac{a_i}{l_i} \right) \phi_i = 1 \quad (29)$$

This expression might be considered as an equation with  $N$  unknown parameters  $l_i$ . An additional assumption is still necessary to determine the cell properties for the polydisperse system. This additional assumption should define the relationship between particle radii and shell thickness for each fraction. We suggest the following simple relationship:

$$l_i = l a_i^n \quad (30)$$

This assumption reduces the number of unknown parameters to only two which are related by the following expression:

$$\sum_{i=1}^N (1 + l a_i^{n-1}) \phi_i = 1 \quad (31)$$

The parameter  $n$  is referred to as a "shell factor". Two specific values of the shell factor correspond to easily understood cases. A shell factor of 0 depicts the case in which the thickness of the liquid layer is independent of the particle size. A shell factor of 1 corresponds to the normal "supersposition assumption" which gives the same relationship between particles and cell radii in the monodisperse case; i.e., each particle is surrounded by a liquid shell which provides each particle the same volume concentration as the volume concentration of the overall system. In general, the "shell factor" might be considered an adjustable parameter because it adjusts the dissipation of energy within the cells. However, our experience using this cell model with acoustics for particle sizing<sup>24</sup> indicates that shell factor equal 1 is almost always suitable. We take this value of  $n$  for the further derivations.

(22) Babchin, A. J.; Chow, R. S.; Sawatzky, R. P. *Electrokinetic measurements by electroacoustic methods*. *Adv. Colloid Interface Sci.* **1989**, *30*, 111.  
 (23) Sawatzky, R. P.; Babchin, A. J. *Hydrodynamics of electroacoustic motion in an alternating electric field*. *J. Fluid Mech.* **1993**, *246*, 321 - 334.  
 (24) Dispersion Technology Inc., Web site: www.dispersion.com.

Substituting the corresponding value of  $b$  into eq 28, we obtain the following expression for the electric field generated by each fraction:

$$\text{CVP}_i = \frac{3\epsilon\epsilon_0\zeta\varphi_i}{K_m a_i(1-\varphi)} \frac{1}{\sin\theta} \frac{\partial u_{i\theta}}{\partial r} \Big|_{r=a} \quad (32)$$

The radial derivative from the tangential velocity contains dependence on the speed of the particle motion in the sound wave according to eq 18:

$$\frac{1}{\sin\theta} \frac{\partial u_{i\theta}}{\partial r} \Big|_{r=a} = \frac{3(u_i - u_m)h(\alpha_i)}{I(\alpha_i)} \quad (33)$$

where  $h$  and  $I$  are special functions given in Appendix 2.

The total CVP value can be calculated as superposition of the fractional CVP<sub>*i*</sub>. The total electroacoustic current equals CVP multiplied by the complex conductivity of the dispersion  $K_s$ :

$$\text{CVI} = \frac{9\epsilon\epsilon_0\zeta K_s(\rho_p - \rho_m)\omega\nabla P}{4K_m\eta(1-\varphi)} \frac{\sum_{i=1}^N \frac{\varphi_i h(\alpha_i)}{\alpha_i I(\alpha_i)(j\omega\rho_p + (\gamma_i/\varphi_i))}}{1 + \frac{\rho_p}{(1-\varphi)\rho_m} \sum_{i=1}^N \frac{\gamma_i}{j\omega\rho_p + (\gamma_i/\varphi_i)}} \quad (34)$$

The particle drag coefficient  $\gamma_i$  was calculated above (eq 17):

$$\gamma_i = -j\omega\varphi_i\rho_m \left( \frac{3H(\alpha_i)}{2I(\alpha_i)} + 1 \right) \quad (35)$$

where

$$\alpha_i = \frac{a_i\sqrt{\omega\rho_m}}{\sqrt{2\eta}}$$

The final expression for CVI of the polydisperse system is the following:

$$\text{CVI} = \frac{9\epsilon\epsilon_0\zeta K_s(\rho_p - \rho_m)\nabla P}{4K_m\eta(1-\varphi)} \frac{\sum_{i=1}^N \frac{\varphi_i h(\alpha_i)}{j\alpha_i I(\alpha_i)(\rho_p - \rho_m)((3H_i/2I_i) + 1)}}{1 - \frac{\rho_p}{1-\varphi} \sum_{i=1}^N \frac{\varphi_i((3H_i/2I_i) + 1)}{\rho_p - ((3H_i/2I_i) + 1)}} \quad (36)$$

where special functions  $h$ ,  $H$ , and  $I$  are given in Appendix 2;  $H_i = H(\alpha_i)$ ,  $I_i = I(\alpha_i)$ .

Figure 3 illustrates graphically the influence of the particle size distribution width on the electroacoustic effect.

This theory has been created for the case of the thin double layer. It can be generalized for the arbitrary double layer thickness following classical papers by Babchin and Sawatzky.<sup>21,22</sup>

**Qualitative Analysis.** We think that it is helpful to create some heuristic understanding of the physical phenomena which take place when an ultrasound pulses passes through a dispersed system. This description

provides answers to some general questions. For instance, why do we need density contrast in the case of ESA when the particles already move relative to the liquid under the influence of an electric field? Why do we need a density contrast to generate CVI at low frequency when the particles already move in phase with the liquid?

As far as we know there are no simple published answers to these questions. To find these answers, we utilize an analogy between sedimentation potential and electroacoustic phenomena. Marlow has used this analogy before,<sup>4</sup> and we will give further justification for this approach.

Let us consider an element of the concentrated dispersed system in the sound wave (Figure 4). The size of this element is selected such that it is much larger than the particle size and also larger than the average distance between particles. As a result, this element contains many particles. At the same time this element is much smaller than the wavelength.

This dispersion element moves with a certain velocity and acceleration in response to the gradient of the acoustic pressure. As a result, an inertia force is applied to this element. At this point we can use the principle of equivalency between inertia and gravity. The effect of the inertia force created by the sound wave is equivalent to the effect of the gravity force.

This gravity force exerts on both particle and liquid inside the dispersion element. Densities of the particles and liquid are different, and forces are different as well. The force acting on the particles depends on the ratio of the densities.

The question arises as to what density should we take into account. To answer this question, let us consider the forces acting on a given particle in the gravity field. The first force is the weight of the particle, which is proportional to its density  $\rho_p$ . This force will be partially balanced by the pressure of the surrounding liquid and other particles. This pressure is equivalent to the pressure generated by an effective medium with density equal to the density of the dispersed system. It becomes clearer when one considers a larger particle surrounded by smaller ones as shown in Figure 4.

We are coming to the well-known conclusion that this force is proportional to the density difference between particle  $\rho_p$  and dispersed system  $\rho_s$ .

It is important to mention here that this force is not necessarily a buoyant force. The last one is proportional to the difference between particle  $\rho_p$  and dispersion medium  $\rho_m$  according to the Archimedes law. Figure 5 illustrates this difference. This figure shows sedimentation of the small spherical cloud of particles in the liquid. Case 1 corresponds to the situation when the cloud settles as one entity and liquid envelopes this settling cloud from outside. Case 2 corresponds to a different case when liquid is forced to move through the cloud. There will be a difference between forces exerting on the particles within the cloud. There is additional force in case 2 caused by liquid pushed through the array of particles.

Electroacoustic phenomena correspond to case 2. This happens because the width of the sound pulse  $W$  is much larger than wavelength  $\lambda$  at high ultrasound frequencies.

$$W \gg \lambda \quad (37)$$

The balance of forces exerted on the particles in a given element of the dispersion consists of the effective gravity force, the buoyancy force, and the friction force related to the filtration of the liquid through the particle array. As a result, particles move relative to the liquid with a speed

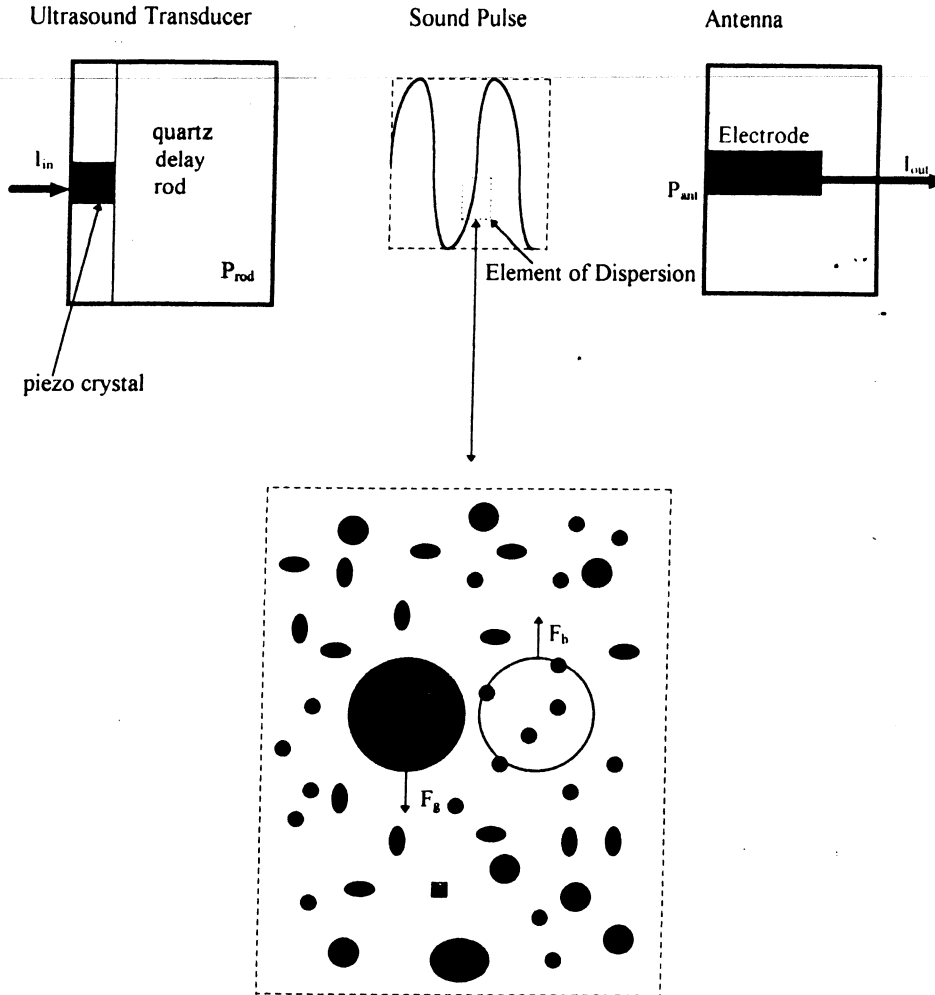


Figure 4. Scheme illustrating design of the electroacoustic sensor and definition of the element of the dispersion.

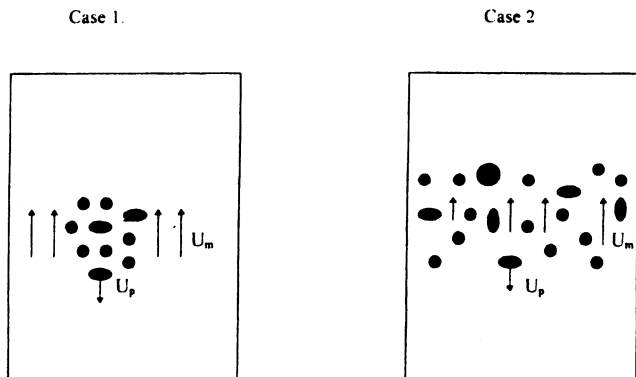


Figure 5. Two possible scenarios for particle sedimentation.

$u_p - u_m$  which is proportional to the density difference between particle and system  $\rho_p - \rho_s$ .

The motion of the particles relative to the liquid disturbs their double layers and as a result generates an electroacoustic signal. This electroacoustic signal is zero when the speed of the particle equals the speed of the medium, which happens when the density of the particle equals the density of the dispersed system. This means that the electroacoustic signal must be proportional to  $\rho_p - \rho_s$ . This conclusion is rather unexpected because O'Brien's relationship makes CVI proportional to  $\rho_p - \rho_m$ .

We can confirm this conclusion using the Onsager principle at the low-frequency limit.

**Low-Frequency Limit.** The Onsager reciprocal relationship follows from the reversibility of time. It links together various kinetic coefficients. This relationship is certainly valid in the stationary case. Much less is known about its validity in the case of alternating field. This means that we can use this relationship only in the limiting case of very low frequency when  $\omega \rightarrow 0$  or at least much lower than the characteristic hydrodynamic frequency  $\omega_{hd}$  and electrodynamic frequencies  $\omega_{ed}$ :

$$\omega \ll \omega_{hd} = \nu/a^2 \quad (38)$$

$$\omega \ll \omega_{ed} = K_m/\epsilon\epsilon_0 \quad \xi_m \gg \xi_c \quad (39)$$

where  $\nu$  is kinematic viscosity,  $\nu = \eta/\rho_m$ ,  $\eta$  is dynamic viscosity,  $a$  is particle radius,  $K_m$  is conductivity of the medium, and  $\epsilon_c$  and  $\epsilon_m$  are dielectric permittivities of the vacuum and medium.

The Onsager relationship provides the following link between quasi-stationary streaming potential CVP, effective pressure gradient which moves liquid relative to the particles  $\nabla P_{rel}$ , electroosmotic current  $\langle I \rangle$ , and electroosmotic flow  $\langle V \rangle$ :

$$\frac{\langle V \rangle}{\langle I \rangle_{\langle \nabla P \rangle = 0}} = \frac{\langle CVP_{\omega=0} \rangle}{\langle \nabla P_{rel} \rangle_{\langle I \rangle = 0}} \quad (40)$$

To use this relationship with respect to CVP, we need to know the effective gradient of pressure. This parameter can be easily obtained following the "coupled phase

model<sup>13-16</sup> for characterizing particle motion in the sound field for a concentrated system. The total friction force exerting on particles equals  $\gamma(u_p - u_m)$ . This force is a part of the pressure gradient which moves particles relative to the liquid. In the extreme case of low frequency eq 5 leads to the following expression for this effective pressure gradient:

$$\nabla P^{\omega=0}_{rel} = \frac{\varphi(\rho_p - \rho_s)}{\rho_s} \nabla P \quad (41)$$

In addition, we can use the obvious fact that the expression in the left-hand side of the eq 40 is the electrophoretic mobility divided by the complex conductivity of the system  $K^*_s$ . As a result, we obtain the following expression for CVI:

$$CVI_{\omega=0} = CVP^* K^*_s = \mu_d \frac{\varphi(\rho_p - \rho_s)}{\rho_s} \nabla P \quad (42)$$

This expression specifies colloid vibration current at the low-frequency limit. It means that  $\mu_d$  is a usual stationary case electrophoretic mobility. We can use the Smoluchowski law for electrophoresis<sup>9</sup> in the form which is valid in concentrated systems:

$$\mu = \frac{\epsilon \epsilon_0 \zeta K_s}{\eta K_m} \quad (43)$$

Here we used two conditions (38) and (39) which restrict applicability of the Smoluchowski law.

A small Dukhin number allows us to apply Maxwell-Wagner theory (eq 20) for expressing conductivity ratio through the volume fraction. As a result, we obtain the following equation for asymptotic value of CVI at low frequency:

$$CVI_{\omega=0} = \frac{\epsilon \epsilon_0 \zeta (1 - \varphi) \varphi (\rho_p - \rho_s)}{\eta (1 + 0.5\varphi) \rho_s} \nabla P \quad (44)$$

This is a very important result because it provides a test for electroacoustic theory. Comparing eq 19 and eq 44, it becomes clear that our new theory satisfies this test because the ratio of the special functions  $I/H$  goes to 0 at low frequency.

At the same time O'Brien's theory does not meet the criterion of the low-frequency transition. Comparison of eq 21 with eq 44 yields the following ratio between O'Brien's theory and the low-frequency asymptotic:

$$\frac{CVI^{\circ}(\omega=0)}{CVI_{\omega=0}} = \frac{(\rho_p - \rho_m) \rho_s}{(\rho_p - \rho_s) \rho_m} = 1 + \frac{\rho_p \varphi}{\rho_m (1 - \varphi)} \quad (45)$$

We test these conclusions with the experiment described in the next section.

## Experiment

The main goal of this experiment is testing the validity of the suggested theory in concentrated systems. Equilibrium dilution is the logical experimental protocol for achieving this goal because it provides a simple criterion of the theory. Equilibrium dilution maintains the same chemical composition of the dispersion medium for all volume fractions. As a result, parameters that are sensitive to the chemistry must be the same for all volume fractions. This means that the  $\zeta$ -potential calculated from CVI is supposed to remain the same for all volume fractions. Variation of  $\zeta$ -potential with volume fraction is an indication that particular theory does not reflect volume fraction dependence properly.

We perform this dilution test with two different dispersions: silica Ludox and rutile R-746 produced by Dupont. We use two different techniques for producing the equilibrium dispersion medium for dilution: dialysis and centrifugation. We perform this experiment with the acoustic and electroacoustic spectrometer DT-1200.<sup>24,25</sup> The next section describes a method of CVI measurement employed by this instrument.

**CVI Measurement.** The electroacoustic spectrometer consists of two parts: the electronic part and the sensor part.

All electronics are placed on two special-purpose boards (signal processor and interface). It also requires a conventional data acquisition card. The signal processor board and DAC are placed inside a personal computer which performs an interface with the user using Windows-95 based software.

The electroacoustic sensor has two parts: a piezoelectric transducer with a critical frequency of 10 MHz and an electroacoustic antenna (Figure 4). There is another design where a sensing electrode is placed on the surface of the transducer. We call this design "electroacoustic probe".

The antenna is designed as two coaxial electrodes separated with a nonconducting rigid ceramic insert. Internal electric impedance between these electrodes can be selected depending on the conductivity range of the samples by means of an internal transformer. The transformer is selected such that the input impedance is significantly less than the external impedance of the sample and the resultant signal is proportional to the short circuit current. This transformer is located just behind the central electrode in order to minimize the stray capacitance.

The transmitting transducer and the receiving antenna are mounted in the opposite walls of the sample chamber such that the gap between the faces is 5 mm.

The signal processor generates the transmit gate which defines the 1 W pulse generated in the interface module as well as the necessary signals to set the frequency. Electroacoustic measurement can be performed either for one frequency or for the chosen set of frequencies from 1 to 100 MHz. The transducer converts these pulses to the sound pulses with some certain efficiency. The sound pulse propagates through the quartz delay rod and eventually through the sample. The acoustic pulse propagating through the sample excites particles and disturbs their double layers. Particles gain dipole moments because of this excitation. These dipole moments generate an electric field. This electric field changes the electric potential of the central electrode of the electroacoustic antenna. The difference of the electric potentials between the central electrode and the external reference electrode causes electric current. This current is registered as colloid vibration current.

The value of this current is very low. It takes averaging of at least 800 pulses in order to achieve the high signal-to-noise ratio. The number of pulses depends on the properties of the colloid. Measurement of CVI in low conducting oil based systems requires averaging of millions of pulses. In principle, this method makes it possible to measure any low-energy signal.

We suggest interpreting this measurement as propagation of the pulse through the transmission line with certain energy losses at different points. This approach allows us to eliminate measurement of the absolute powers. We simply compare pulse intensity before and after transmission and take into account all internal energy losses. This idea is accomplished as described below.

At the beginning of the each measurement the interface routes the pulses to a reference attenuator channel consisting of a fixed 40 dB attenuator and similarly routes the output of this precision attenuator to the input section of the signal processor. Since the precision attenuator has a known response over the entire frequency range, this step allows us to characterize all energy losses in the measuring circuits at each frequency.

The next step in the measurement is to determine the losses in the electroacoustic sensor. The signal processor now commands the interface to substitute the electroacoustic sensor for the reference attenuator. The 1 W pulses are now sent to the

(25) Dukhin, A. S.; Goetz, P. J. Method and device for characterizing particle size distribution and zeta potential in a concentrated system by means of Acoustic and Electroacoustic Spectroscopy. US Patent, pending.

transmitting transducer, which converts these electric pulses to sound pulses. We have certain energy losses at this point. This loss depends on the transducer efficiency and is pretty much constant.

The sound pulses propagate through the quartz delay rod (see Figure 4) and eventually reach the surface of the transducer which faces dispersion. It loses some energy at this point because of the reflection caused by mismatch of the acoustic impedances of the delay rod ( $Z_{tr}$ ) and dispersed system ( $Z_s$ ).

Some part of the pulse passes into the gap between the transducers which is filled with the dispersion under test and propagates through it. It loses energy during propagation due to the attenuation.

At last this sound pulse reaches the electroacoustic antenna which converts it back to an electrical signal. This conversion is also related to energy losses.

This final electric pulse is routed through the interface to the input signal port on the signal processor where the signal level of the acoustic sensor output is measured. Comparison of the amplitude and phase of the electroacoustic sensor output pulse with that of the reference channel output pulse allows the program to calculate precisely the overall loss in the sensor at each frequency.

Experimental output of the electroacoustic sensor  $S_{exp}$  is the ratio of the intensity of the input electric pulse to the transducer  $I_{in}$  to the output electric pulse in the antenna  $I_{out}$  (Figure 4):

$$S_{exp} = I_{out}/I_{in} \quad (46)$$

The intensity of the input electric pulse is related to the intensity of the sound pulse in the delay rod through some constant  $C_{tr}$ , which is a measure of the transducer efficiency and energy losses at this point:

$$I_{rod} = C_{tr}I_{in} \quad (47)$$

The intensity of the sound in the delay rod is proportional to the square of the sound pressure, here  $P_{rod}$ :

$$P_{rod} = \sqrt{2\rho_{rod}c_{rod}C_{tr}I_{in}} \quad (48)$$

where  $\rho_{rod}$  and  $c_{rod}$  are density and sound speed of the rod material.

At the other end we can use definition of the electric pulse intensity as a square of the electric current in the antenna, which is CVI:

$$I_{out} = (CVI)^2 C_{ant} \quad (49)$$

where the constant  $C_{ant}$  depends on a geometrical factor of the CVI space distribution in the vicinity of the antenna and electric properties of the antenna only for the proper ratio of the electric impedances of the antenna and dispersed system.

Substituting eq 49 into eq 46, we obtain the following expression relating CVI to the measured parameter  $S_{exp}$ :

$$CVI/P_{rod} = \sqrt{S_{exp}/2\rho_{rod}c_{rod}C_{tr}C_{ant}} \quad (50)$$

The value of CVI depends on the pressure near the antenna surface  $P_{ant}$ . This pressure is lower than pressure in the rod  $P_{rod}$  because of the reflection losses on the rod surface and attenuation of the pulse in the dispersion. There are two ways to take into account these effects. We can either measure corresponding losses using reflected pulses or we can calculate these losses. If we choose the second way, we should use the following corrections:

$$P_{ant} = P_{rod} \frac{2Z_s}{Z_s + Z_{rod}} \exp\left(-\frac{\alpha L}{2}\right) \quad (51)$$

where  $\alpha$  is attenuation of the sound intensity expressed in neper per centimeter and  $L$  is the distance between transducer and antenna in centimeters. These corrections lead to the following expression for CVI:

$$\frac{CVI}{P_{ant}} = \sqrt{S_{exp}/2C_{ant}C_{tr}\rho_{rod}c_{rod}} \frac{Z_s + Z_{rod}}{2Z_s} \exp\left(\frac{\alpha L}{2}\right) \quad (52)$$

The gradient of pressure  $\nabla P$  in the eq 19 for CVI equals the gradient of the pressure  $P_{ant}$ . Using this fact and substituting CVI from eq 52, we obtain the following equation relating properties of the dispersion to the measured parameter  $S_{exp}$ :

$$\frac{3\epsilon\epsilon_0\zeta(1-\varphi)\varphi(\rho_p - \rho_s)}{2\eta(1+0.5\varphi)} \frac{\rho_p}{\rho_s} G(a,\varphi) = \frac{cC_{cal}}{f} \left(1 - i\frac{\alpha c}{2\omega}\right) \sqrt{S_{exp}} \frac{Z_s + Z_{rod}}{2Z_s} \exp\left(\frac{\alpha L}{2}\right) \quad (53)$$

where  $c$  is sound speed in the dispersion,  $f$  is frequency in hertz, and

$$G(a,\varphi) = \frac{H + [I/(1-\varphi)]}{1.5H - \frac{(1-\varphi)\rho_p - \rho_s}{\rho_s} I}$$

In the case of the polydisperse system we should use eq 36 for expressing CVI in eq 52.

Equation 53 contains the unknown calibration constant  $C_{cal}$  which is independent of the properties of the dispersion. This constant can be calibrated out using calibration with the known colloid. We use for this purpose silica Ludox at 10 wt % diluted with  $10^{-2}$  mol/L KCl. These silica particles have  $\zeta$ -potential of  $-38$  mV at pH 9.3.

Expression 53 can be used for calculating either  $\zeta$ -potential only in the case of a single frequency measurement or both  $\zeta$ -potential and particle size in the case of multiple frequencies.

The new theory yields a new range of the frequencies. This theory predicts that critical frequency becomes higher with increasing volume fraction. This is seen from the graphs in Figure 2. Computer computation shows that this shift is about 1 order of magnitude for 40% volume fraction. This means that the optimum frequency range according to the new theory is

$$v/a^2 < \omega < 40v/a^2 \quad (54)$$

if we want to cover volume fractions up to 40%.

**Materials and Experimental Protocol.** We used silica Ludox and rutile R-746 from Dupont for this experiment.

Selection of the silica Ludox is related to the small size of the particles. This allows us to eliminate any particle size dependence in eq 53 because  $G(a,\varphi) = 1$  for small particles. Using small particles gives one more simplifying advantage: it eliminates contribution of attenuation because small particles do not attenuate sound at low frequency. This means that the choice of small particles allows us to test volume fraction dependence only. It is important because this dependence is the most pronounced difference between different theories.

Silica Ludox TM satisfies all specified conditions because its nominal particle size reported by DuPont is about 22 nm. We measure the size using acoustics. It is quite close to the nominal value as will be shown below. At the same time particle size should not be too small for the given ionic strength in order to satisfy the thin double layer restriction (eq 1.3). Silica Ludox meets this requirement because of the relatively high ionic strength about 0.1 mol/L. Otherwise we would have to generalize the theory removing the thin double layer restriction following Babchin et al. papers.<sup>22,23</sup>

Selection of rutile as the second dispersion gives us an opportunity to test particle size dependence and enhance the density contrast contribution. We used rutile R-746 produced by E. I. DuPont de Nemours. This product was a concentrated stable dispersion with 76.8 wt % solids. We took 100 mL of this dispersion and weighed it. This weight was 234 g, which yields particle material of 3.9 g/cm<sup>3</sup> average density. This density was somewhat lower than the density of the regular rutile, perhaps because of the stabilizing additives.

Equilibrium dilution protocol requires a pure solvent which is identical with the medium of the given dispersed system. In

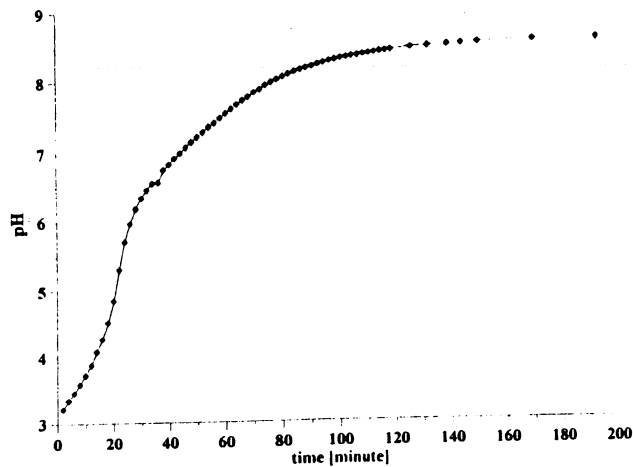


**Figure 6.** Kinetic curve describing variation of pH in the external dialysis solution versus time for silica Ludox.

principle one can try to separate the dispersed phase and dispersion medium using either sedimentation or centrifugation. This method does not work for silica Ludox because the particle size is too small.

The other way to create an equilibrium solution for silica Ludox is dialysis. We used this one. Dialysis allows us to equilibrate the dispersion medium with external solution over some period of time. We used regenerated cellulose tubular membrane Cell\*Sept4 with pore size 12 000–14 000 Da. The external solution was  $10^{-1}$  mol/L KCL with pH adjusted to 9.5 using hydrochloric acid. Membrane filled with silica Ludox was placed inside the KCl solution which was continuously mixed with a magnetic stirrer. We made two samples in order to check reproducibility.

In addition we prepared another setup using KCl solution with pH 3. This setup allowed us to estimate the equilibration time. The initial pH of the silica Ludox is about 9 at 23 °C. We monitored the change of the pH in the external solution. The corresponding kinetic curve is shown in Figure 6. It is seen that pH becomes 8.6 after 3 h of equilibration. This was close to the final pH value of 8.7 after 12 days of equilibration. We waited 12 days because equilibration time depends on the diffusion coefficient, which is highest for H ions. The higher diffusion coefficient, the lower the equilibration time.

Before starting dilution we checked again the weight fraction of the silica Ludox using a pycnometer. We were concerned about losing silica particles through the membrane pores into the solution. The weight fraction remained unchanged, which means that the pores were too small for silica particles.

We had two sets of 50% silica with corresponding equilibrium solution. This allowed us to check two ways of dilution. We used one set for diluting from the high weight fraction down. We did this adding solution to the dispersed system. We used the opposite procedure with the other sample. We added dispersed system to the solution.

In the case of rutile we used centrifugation of the initial 76.8 wt % dispersion in order to create equilibrium supernate. We used this supernate for preparing equilibrium 1.1 vol % rutile dispersion diluting the initial dispersion. After measurement with this dilute system, we added more initial dispersion for preparing the next volume fraction: 3.2 vol %. We proceeded this way making a more and more concentrated system. All together 11 different volume fractions from 1.1 to 45.9 vol % were tested (see Figure 8).

For each volume fraction we measured attenuation spectra, sound speed, pH, conductivity, temperature, magnitude, and phase of CVI.

Attenuation spectra were measured in the frequency range from 3 to 100 MHz, sound speed at 10 MHz, conductivity at 3 MHz, magnitude of CVI at 3 MHz, and phase of CVI at 1.5 MHz. Some of the results are discussed below.

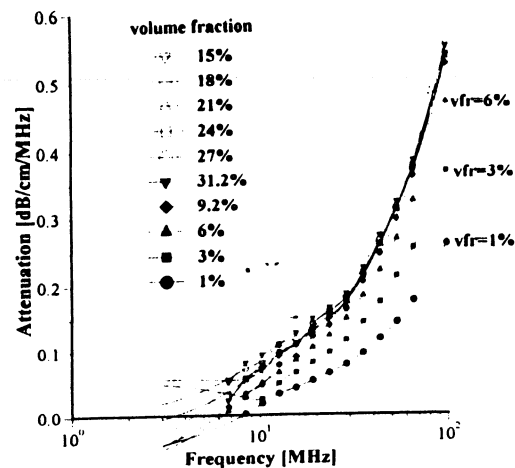


**Figure 7.** Attenuation spectra measured for silica Ludox TM at different volume fractions.

## Results and Discussion

Measured attenuation spectra are shown in Figures 7 and 8. The attenuation for silica Ludox is much lower than that for rutile. This happens because of the smaller size and lower density contrast for silica. Attenuation spectra of silica become almost indistinguishable at volume fraction above 9%. This reflects a nonlinear dependence of the attenuation on the volume fraction. This nonlinearity appears because of the particle–particle interaction. This interaction shifts critical frequency to the higher values.

This peculiarity of the attenuation spectra was known before.<sup>15</sup> It is even more pronounced for rutile (Figure 8). Attenuation at low frequency decreases with increasing volume fraction above 16.6 vol %. It is exactly the same effect that makes attenuation constant for silica.

Existing theory takes into account this nonlinear effect. As a result, particle size calculated from this attenuation spectra is almost constant for all volume fractions for both silica and rutile (Figure 9). A slight increase at high volume fraction can be caused by aggregation. It is important to mention here that the dilute case theory would yield size decreasing dramatically with volume fraction.

It is seen that our size is somewhat larger than nominal. Perhaps the difference from nominal value is caused by a different technique applied by Dupont for characterizing the size of these particles. It is also clear that nominal size corresponds to the dilute system whereas we measured size for the concentrated one.

It is seen (Figure 7) that attenuation for silica at 3 MHz is negligible indeed. This means that our expectations to eliminate this contribution to the CVI measurement using small particles were true.

At the same time we have appreciable attenuation for rutile at 3 MHz. This gives us a chance to verify the way we correct CVI for sound attenuation (eq 53).

The sound speed of the silica Ludox dispersion varies only within 2% for weight fraction changing from 1 to 50% (see Figure 10). It eliminates contribution from the changing of the acoustic impedance to the measured CVI for silica as well.

Figures 11 and illustrate the main results of this paper. They give  $\zeta$ -potential calculated from the measured CVI using various theoretical models. Only our new theory yields a  $\zeta$ -potential that remains almost the same within the complete volume fraction range. Variations do not exceed 10%.

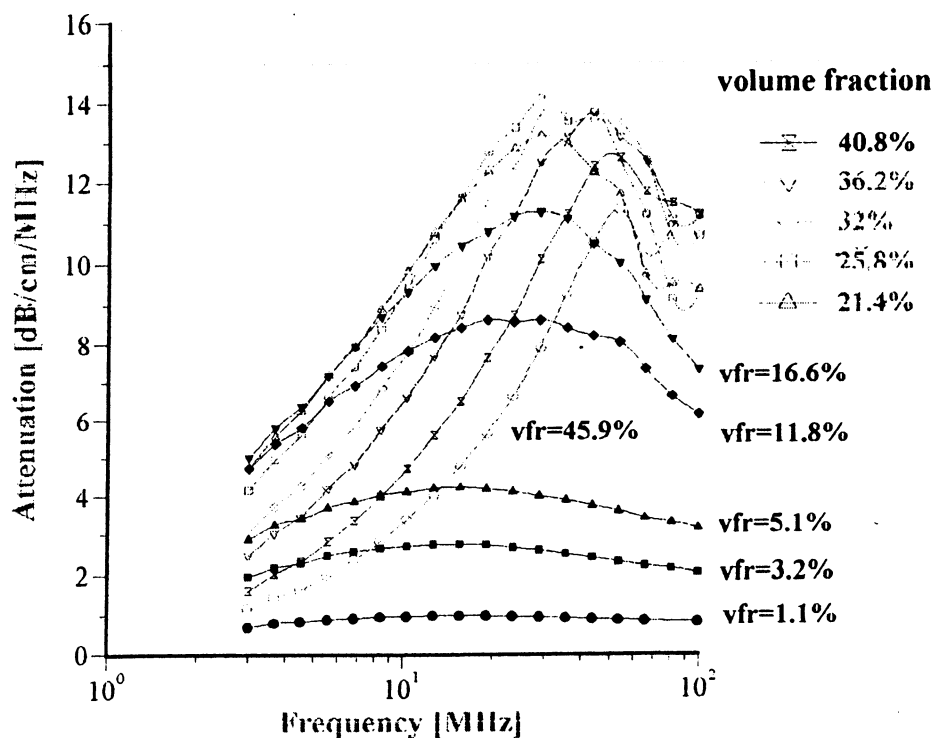


**Figure 8.** Attenuation spectra measured for rutile R-746 at different volume fractions.

At the same time “hybrid O’Brien’s theory” produces a big drop in the  $\zeta$ -potential at high volume fraction. This theory is the combination of O’Brien’s relationship and our cell model theory for dynamic electrophoretic mobility. In the case of rutile error reaches 300% at volume fraction of 45.9%.

Similar results for silica allow us to conclude that the reason for this erroneous  $\zeta$ -potential drop is O’Brien’s relationship but not our theory for the dynamic mobility. Our theory reduces in this case to the Smoluchowski law. It is O’Brien’s relationship which brings about 100% error in  $\zeta$ -potential for silica at 30 vol %.

The situation becomes even worse for the original O’Brien theory combined with the Levine cell model. In principle we are able to apply the original O’Brien theory as it is presented in the patent<sup>7</sup> with the Levine cell model. However, instead of recovering these complicated mathematical expressions, we decided just to show the effect of the missing volume fraction dependence. It is known<sup>5</sup> that the Levine cell model lacks the multiplier  $K_s/K_m$  compared to the Shilov–Zharkikh cell model.<sup>19</sup> This difference is a major factor distinguishing “O’Brien–Levine theory” and “hybrid O’Brien theory” for this particular dispersion. These theories have different particle size dependence, but in the case of relatively small particles this difference is not very important. However, we neglect difference in particle size dependence and take into account only different volume fraction effects. The last curves marked as “O’Brien–Levine theory” illustrate results produced by this theory within the scope of the above-mentioned assumption of the same particle size dependence for two theories.

### Conclusions

We have derived a new electroacoustic theory without using O’Brien’s relationship between electroacoustic signal and dynamic electrophoretic mobility. Instead we use the coupled phase model and the cell model concept. We

manage to extend this theory to polydisperse systems without using superposition assumption for the hydrodynamic part of the problem. This new theory is supposed to be valid for polydisperse concentrated dispersions with low surface conductivity and thin double layer.

The new theory gives the same result as O’Brien’s theory in the dilute system. At the same time this new theory predicts quite different values of the electroacoustic signal in concentrated systems.

We have shown that our new theory satisfies Onsager’s and Smoluchowski’s principles at low frequency at any volume fraction.

At the same time the “hybrid O’Brien’s theory”, which employs O’Brien’s relationship and the cell model theory for the dynamic electrophoretic mobility, does not meet Onsager’s and Smoluchowski’s principles at low frequency for concentrated systems. We came to the conclusion that this happens because of O’Brien’s relationship.

We have tested both theories with an equilibrium dilution experiment using silica Ludox and rutile R-746 from Dupont.

The test with silica Ludox TM confirmed that our theory gives correct volume fraction dependence within a whole available range of the volume fraction up to 30 vol %, whereas O’Brien’s relationship leads to significant (100%) deviation from the experimental data.

The equilibrium dilution test with the stable rutile dispersion proved that our theory gives the correct particle size dependence within volume fraction ranging from 1.1 to 45.9 vol %, as well as volume fraction dependence. We have shown that this new theory yields almost constant  $\zeta$ -potential ( $\pm 10\%$  variation) within the whole volume fraction range. Polydispersity of the rutile sample was not a significant factor, at least in comparison with volume fraction and particle size.

We also calculated  $\zeta$ -potential using “hybrid O’Brien’s theory” which employs O’Brien’s reciprocal relationship and our cell model theory for electrophoretic dynamic

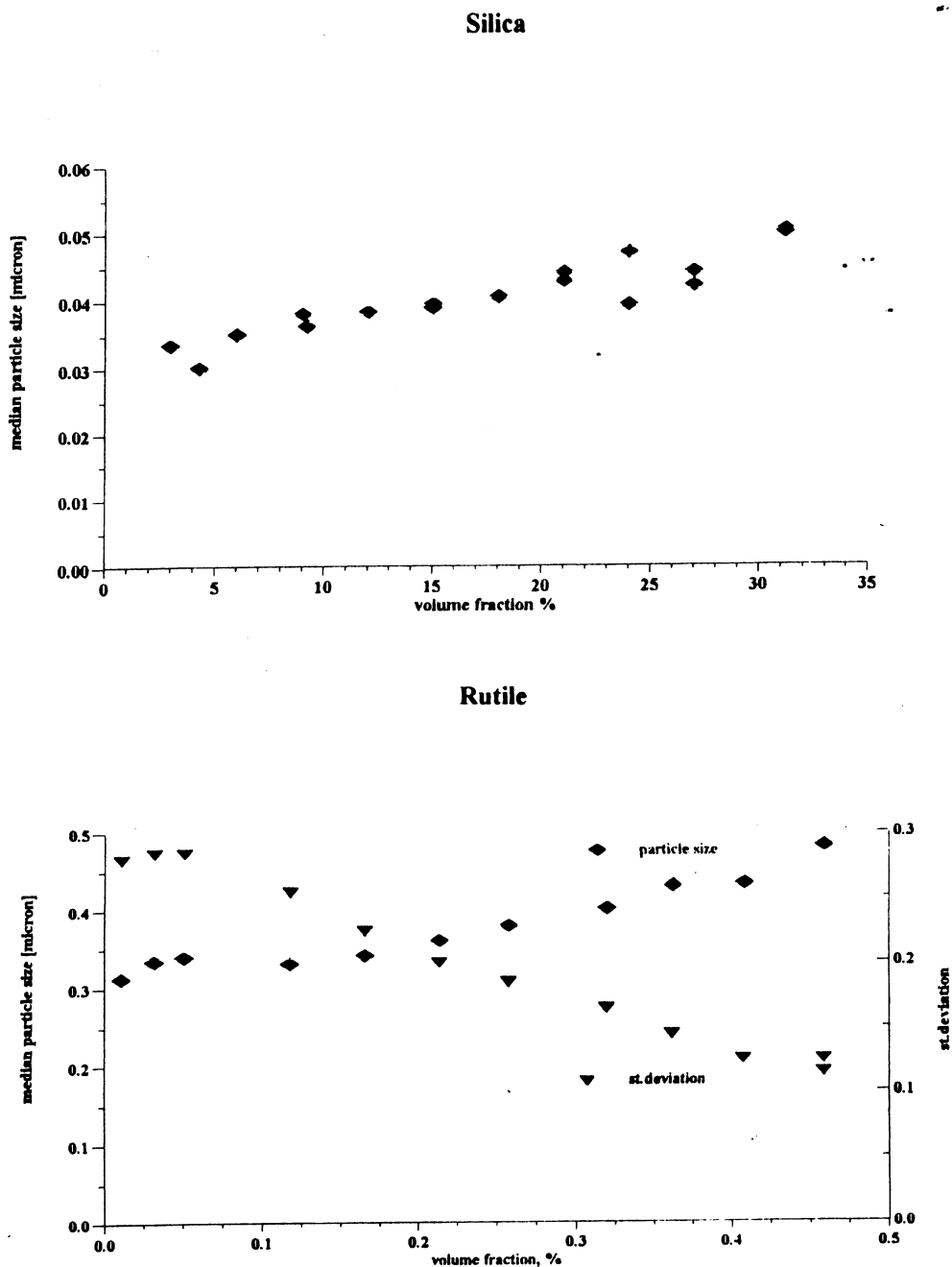


**Figure 9.** Median particle size of silica and rutile calculated from the attenuation spectra of Figures 7 and 8.

mobility.<sup>9-11</sup> This theory produces  $\zeta$ -potential about 4 times smaller (300% error) than expected at the highest volume fraction of 45.9 vol %.

There is some reason to believe that the situation would be even worse for the original O'Brien theory with Levine cell model. It misses an additional volume fraction dependence related to the conductivity ratio. If we take into account only volume fraction effect and neglect particle size dependence for dynamic electrophoretic mobility, error reaches almost 1000%.

We would like to stress that our new electroacoustic theory has been created so far for CVI only. It is not clear yet how to apply it to ESA effects. Required modifications will depend on the design of the instrument including ratio of masses of the chamber and the sample. This ratio determines an appropriate frame of reference. At the same time the basic physical framework should work for ESA effect as well as for CVI.

We would also like to stress that to our knowledge the commercially available electroacoustic spectrometer based on the ESA principle, the Acoustosizer of Colloidal Dynamics, applies an empirical correction for calculating  $\zeta$ -potential from the ESA signal. This follows directly from the recent review published by Prof. Hunter, who is one of the Acoustosizer authors.<sup>1</sup> This correction is necessary because, as Prof. Hunter admits, their theory was valid only up to 5 vol %. This empirical correction works and reduces dramatically the error of the Acoustosizer in some concentrated systems. Unfortunately, this empirical correction masks results of theoretically justified calculations.

#### Appendix 1. CVI as a Streaming Current

We will use the cell model for describing the relationship between macroscopic electric field strength (CVP) and local electric potential distribution  $\phi$  within a cell. According to this model we equally redistribute liquid between

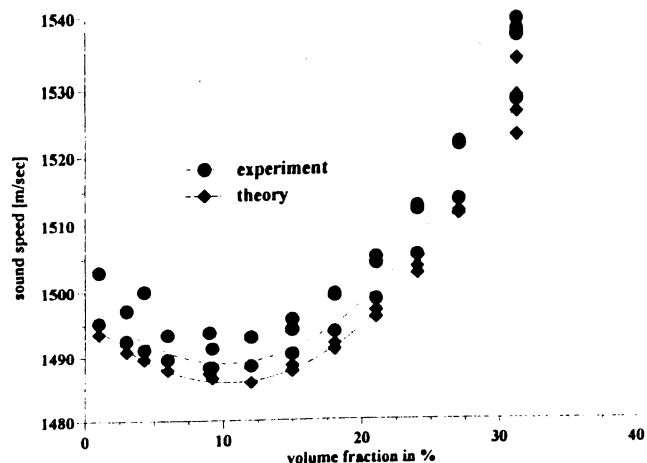


Figure 10. Sound speed of silica Ludox TM versus volume fraction measured and calculated.

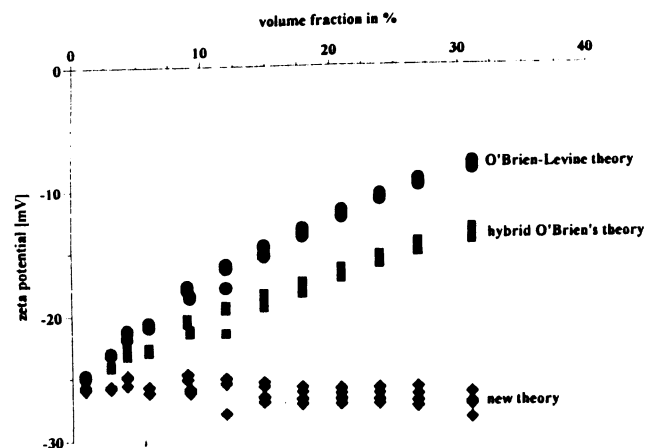


Figure 11. Electrokinetic  $\zeta$ -potential calculated from the measured CVI at various volume fractions using different electroacoustic theories for silica Ludox.

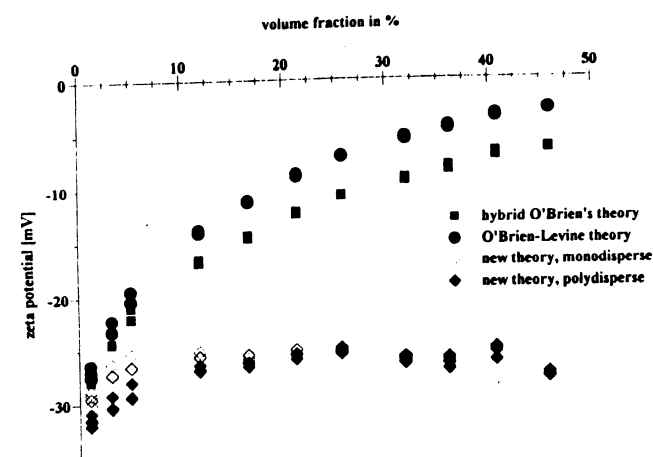


Figure 12. Electrokinetic  $\zeta$ -potential calculated from the measured CVI at various volume fractions using different electroacoustic theories for rutile R-746 from Dupont.

particles and assume that liquid associated with each particle creates a spherical cell of radius  $b$ . This radius is related to the particle radius according to the following expression:

$$b^3 = a^3/\varphi \quad (1.1)$$

We prefer to use the Shilov-Zharkikh cell model<sup>18</sup> over the Levine one.<sup>4</sup> All arguments for this decision are given in ref 8.

According to the Shilov-Zharkikh cell model macroscopic electric field and local electric potential are related by the following expression:

$$\text{CVP} = -\frac{f(r=b)}{b \cos \theta} \quad (1.2)$$

We will calculate electric potential within a cell using two simplifications. We assume that the double layer thickness must be much smaller than particle radius  $a$ :

$$\kappa a \gg 1 \quad (1.3)$$

where  $\kappa$  is reciprocal Debye length.

It is possible to eliminate this restriction in the future following well-known papers by Babchin et al.<sup>21,22</sup>

The second simplification requires a surface conductivity  $\kappa''$  contribution to be negligibly small. This happens when the dimensionless Dukhin number  $Du$  introduced by Lyklema<sup>19</sup> is sufficiently small:

$$Du = \frac{\kappa''}{K_m a} \ll 1 \quad (1.4)$$

This case is very representative. It covers almost all aqueous systems.

The condition of the thin double layer allows us to describe distribution of the electric potential  $\phi$  with the Laplace equation:

$$\Delta \phi = 0 \quad (1.5)$$

The general spherical symmetrical solution of this equation

$$\phi = -Er \cos \theta + \frac{d}{r^2} \cos \theta \quad (1.6)$$

contains two unknown constants  $E$  and  $d$ . Two boundary conditions are required for calculating these constants.

**Surface Boundary Condition.** This boundary condition reflects continuity of the bulk current  $I$  and surface current  $I_\theta$

$$-K_m \nabla_n \phi = -\text{div}_s I_\theta \quad (1.7)$$

There is only one essential component in the surface current when the double layer is thin and surface conductivity is low. It is caused by hydrodynamic involvement of the electric charge  $\rho_{dl}$  in the diffuse layer:

$$I_\theta = \int_0^\pi \rho_{dl}(x) u_\theta(x) dx \quad (1.8)$$

We consider double layer as a flat which is obviously true in the considered case of the thin double layer. The distance from the particle surface is  $x$ .

We can apply Taylor expansion to the tangential speed  $u_\theta$  near the particle surface:

$$u_\theta(x) = u_\theta(x=0) + x \frac{\partial u_\theta}{\partial x} \Big|_{x=0} \quad (1.9)$$

The first term equals 0 because liquid does not slide relative to the particle on the particle surface. As a result, surface current within the thin double layer can be expressed as follows:

$$I_s = \frac{\partial u_\theta}{\partial x} \Big|_{x=0} \int_0^\pi \rho_{dl}(x) x dx \quad (1.10)$$

At this point we imply again a peculiarity of the thin double layer. There is a known relationship between electric charge density in the double layer and  $\zeta$ -potential:

$$\int_0^\infty \rho_{dl}(x) x dx = -\epsilon\epsilon_0\zeta \quad (1.11)$$

Surface current equals

$$I_s = -\epsilon\epsilon_0\zeta \frac{\partial u_\theta}{\partial r} r=a \quad (1.12)$$

Substitution of eq 1.12 into eq 1.7 yields the first boundary condition.

**Cell Boundary Condition.** The cell boundary condition specifies the values of the normal derivative of the electric potential on the cell surface:

$$\frac{\partial \phi}{\partial r} r=b = 0 \quad (1.13)$$

**CVP Value.** To find CVP, we should calculate unknown constants  $E$  and  $d$  using eq 1.13, substitute these constants into the general solution for  $\phi$ , calculate the value of  $\phi$  at  $r = b$ , and substitute this result into eq 1.2. As a result, we have the following expression for CVP:

$$\text{CVP} = \frac{3\epsilon\epsilon_0\zeta}{K_m a} \frac{a^3}{b^3 - a^3} \frac{1}{\sin \theta} \frac{\partial u_\theta}{\partial r} r=a \quad (1.14)$$

This expression relates CVP to the yet unknown derivative of the tangential component of the liquid motion relative to the particle surface.

## Appendix 2. Special Functions

There are several special functions used in this theory. They are specified as follows:

$$H(\alpha) = \frac{ih(\alpha)}{2\alpha} - \frac{i}{2} \frac{dh(x)}{dx} x=\alpha$$

$$h(x) = h_1(x) h_2(\beta) - h_1(\beta) h_2(x)$$

$$I = I(\beta) - I(\alpha)$$

$$I(x) = I_1(x) - I_2(x)$$

$$I_1(x) =$$

$$-h_1(\beta) \exp(x(1+i)) \left[ \frac{3(1-x)}{2\beta^3} + i \left( \frac{x^2}{\beta^3} - \frac{3x}{2\beta^3} - \frac{1}{x} \right) \right]$$

$$I_2(x) =$$

$$-h_2(\beta) \exp(x(1+i)) \left[ \frac{3(1+x)}{2\beta^3} + i \left( \frac{x^2}{\beta^3} + \frac{3x}{2\beta^3} - \frac{1}{x} \right) \right]$$

$$h_1(x) =$$

$$\frac{\exp(-x)}{x} \left[ \frac{x+1}{x} \sin x - \cos x + i \left( \frac{x+1}{x} \cos x + \sin x \right) \right]$$

$$h_2(x) =$$

$$\frac{\exp(x)}{x} \left[ \frac{x-1}{x} \sin x + \cos x + i \left( \frac{1-x}{x} \cos x + \sin x \right) \right]$$

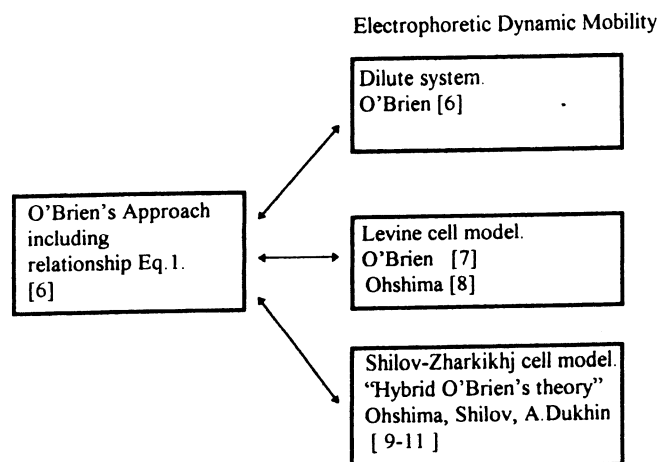
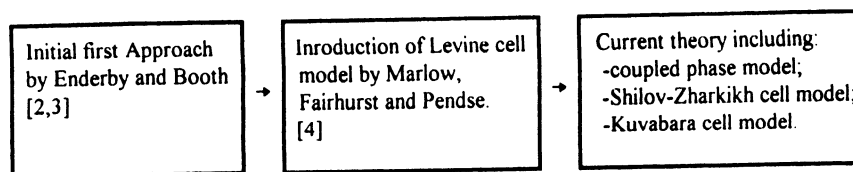


**Figure 1.** Block scheme illustrating various versions of electroacoustic theory.

particle size, and frequency is incorporated into dynamic electrophoretic mobility. The coefficient of proportionality between  $ESA(CVI)$  and  $\mu_d$  is frequency independent as well as independent of particle size and  $\zeta$ -potential. This peculiarity of eq 1 made dynamic electrophoretic mobility a central parameter of the electroacoustic theory.

The first theory of the dynamic electrophoretic mobility which relates this parameter to other properties of the dispersed system was created initially by O'Brien for the dilute case only, neglecting particle-particle interaction. We call this version the "dilute O'Brien's theory".

Later he applied the Levine cell model trying to expand dynamic electrophoretic theory to concentrated systems.<sup>7</sup> This work was generalized recently by Ohshima.<sup>8</sup> We call this version the "O'Brien-Levine" theory.

The last development of this approach was made recently by Ohshima, Shilov, and A. Dukhin.<sup>9-11</sup> We used the Shilov-Zharkikh cell model for dynamic electrophoretic mobility. We call the combination of O'Brien's relationship and our dynamic electrophoretic mobility theory the "hybrid O'Brien's theory".

(4) Marlow, B. J.; Fairhurst, D.; Pendse, H. P. Colloid Vibration Potential and the Electrokinetic Characterization of Concentrated Colloids. *Langmuir* **1983**, *4*, 3, 611-626.

(5) Levine, S.; Neale, G. H. The Prediction of Electrokinetic Phenomena within Multiparticle Systems. I. Electrophoresis and Electroosmosis. *J. Colloid Interface Sci.* **1974**, *47*, 520-532.

(6) O'Brien, R. W. Electro-acoustic Effects in a dilute Suspension of Spherical Particles. *J. Fluid Mech.* **1988**, *190*, 71-86.

(7) O'Brien, R. W. Determination of Particle Size and Electric Charge. US Patent 5,059,909, Oct 22, 1991.

(8) Ohshima, H. Dynamic Electrophoretic Mobility of Spherical Colloidal Particles in Concentrated Suspensions. *J. Colloid Interface Sci.* **1997**, *195*, 137-148.

(9) Dukhin, A. S.; Shilov, V. N.; Borkovskaya, Yu. Dynamic Electrophoretic Mobility in Concentrated Dispersed Systems. Cell Model. *Langmuir* **1995**, *15*, 3452-3457.

(10) Dukhin, A. S.; Ohshima, H.; Shilov, V. N.; Goetz, P. J. Electroacoustics for Concentrated Dispersions. *Langmuir* **1999**, *15*, 3445-3451.

(11) Ohshima, H.; Dukhin, A. Colloid Vibration Potential in a Concentrated Suspension of Spherical Colloidal Particles. *J. Colloid Interface Sci.* **1999**, *212*, 449-452.

Figure 1 is a block scheme of the various versions of the electroacoustic theory and helps to understand this somewhat complicated situation.

For a time, it looked like O'Brien's approach had won out over the other approach because it appeared to yield a desirable electroacoustic theory for the concentrated case. However, one important question remains unanswered. In principle these two approaches must give the same result. It is not clear if this is the case. These two approaches are completely independent and the relationship between them is not known even in the dilute case.

It is obvious that such a comparison must be done. It would provide strong support for O'Brien's theory if the comparison confirms that the two approaches merge. The first approach is somewhat more basic. It needs only major well-tested electrokinetic equations.

To perform the comparison, we need a version of the first approach theory which would be valid for the same conditions as O'Brien's theory, including our recent generalization for dynamic electrophoretic mobility. The development of such a theory is a goal of this paper.

We restrict consideration with the simpler case of the CVI and/or CVP (colloid vibration potential) when the gradient of pressure is a driving force generating the electroacoustic signal. We would like to be cautious concerning expanding this new theory to the ESA phenomenon. It turns out that the problem of frame of references has different implications for these different electroacoustic effects.

We will use a "coupled phase model"<sup>13-16</sup> for describing the speed of the particle relative to the liquid. The

(12) Ohshima, H. Sedimentation Potential in a Concentrated Suspension of Spherical Colloidal Particles. *J. Colloid Interface Sci.* **1998**, *208*, 295-301.

(13) Harker, A. H.; Temple, J. A. G. Velocity and Attenuation of Ultrasound in Suspensions of Particles in Fluids. *J. Phys. D.: Appl. Phys.* **1998**, *21*, 1576-1588.

(14) Gibson, R. L.; Toksoz, M. N. Viscous Attenuation of Acoustic Waves in Suspensions. *J. Acoust. Soc. Am.* **1989**, *85*, 1925-1934.

Kuvabara cell model yields the required hydrodynamic parameters such as the drag coefficient. We connect this parameter with the generated electric field using the Shilov-Zharkikh cell model.<sup>19</sup> We have derived this new electroacoustic theory initially for the monodisperse case and then generalized it for polydispersity without using the superposition assumption.

We compared the new theory with "hybrid O'Brien's theory" and came to the conclusion that they are different. Which one is correct?

There is an opportunity to derive an independent expression for CVI in the quasi-stationary limit using the Onsager relationship and the Smoluchowski law. We use this opportunity and show that our new theory satisfies the transition requirement to the quasi-stationary limit at any volume fraction, whereas the O'Brien theory does only in dilute systems.

This situation resembles somewhat the problem of the sedimentation potential. There is a simple way to create a theory of sedimentation potential using the Onsager reciprocal relationship. However, it turned out that straight derivation rooted down to the basic physical equations is also very helpful. In the case of the sedimentation potential, such a derivation performed by Ohshima<sup>12</sup> provides an important background and confirmation for Onsager-based theory.

Failure of the O'Brien relationship to satisfy the Onsager principle is very unfortunate for electroacoustic theory because it prevents us from using a very convenient eq 1 and notion of dynamic electrophoretic mobility.

We realize the importance of this conclusion. It is clear that such strong statements must be proved with experiment. We have performed this test here using an equilibrium dilution of silica Ludox TM and rutile R-746 produced by Dupont.

The choice of small silica Ludox particles (30 nm) allowed us to test O'Brien's relationship by itself, eliminating particle size dependence. Basically, this test targeted only volume fraction dependence. It turned out to be wrong in O'Brien's theory and correct in our new theory.

The next logical step to test the theory would be implementing particle size dependence into the experiment. Actually, we had made an experiment of this kind once before when we tried to test our cell model theory of dynamic electrophoretic mobility.<sup>10</sup> We used rutile R-900 at low pH for equilibrium dilution protocol. We managed to make the  $\zeta$ -potential almost constant for all volume fractions using an additional multiplier  $(1 - \varphi)$ , where  $\varphi$  is volume fraction. We attributed this multiplier to the problem of the frame of references. Our new theory gives completely new justification to this multiplier. It is clear now that this multiplier appears because we should use the density contrast between particle and system ( $\rho_p - \rho_s$ ) instead of O'Brien's version of the density contrast between particle and medium ( $\rho_p - \rho_m$ ).

There is one more factor contributing to the constant value of  $\zeta$ -potential in our old experiment. We took into

account reflection of sound using intensity of sound instead of the gradient of pressure. It was mistakenly done in the old DT software. The new procedure is described in this paper. This mistake was another fortunate compensating factor.

To our regret it is impossible to recalculate our old experiment using new theory because the wrong correction for reflection affects calibration as well. However, it is clear that we should not expect significant changes because of the mentioned two fortunately used but wrongly justified factors.

In addition, we are not satisfied with the way we performed that experiment. We prepared dispersion by ourselves relying completely on the electrostatic factor of stability. We used just low pH effect causing high surface charge. Afterward we used sedimentation in order to separate particle and supernate. It is not the most reliable way to do this. Centrifugation is much better.

Taking into account these mistakes of our first experience with equilibrium dilution, we decided to perform a completely new test which would be particle size sensitive. This time we chose the initially stable commercially available dispersion of rutile R-746 produced by Dupont.

This equilibrium dilution test confirms again our theory this time including particle size dependence. It also shows that O'Brien's relationship leads to hundreds percents of error at high volume fractions.

We would like to stress that according to our knowledge the commercially available electroacoustic spectrometer based on ESA principle, the Acoustosizer of Colloidal Dynamics, applies an empirical correction for calculating  $\zeta$ -potential from the ESA signal. This follows directly from the recent review published by Prof. Hunter, who is one of the Acoustosizer authors.<sup>1</sup> The correction is necessary because, as Prof. Hunter admits, their theory is valid only up to 5 vol %. This empirical correction works and dramatically reduces Acoustosizer error in some concentrated systems. Unfortunately, this empirical correction masks results of theoretically justified calculations.

## Theory

**Frame of Reference.** When sound is the driving force (CVI or CVP), the correct inertial frame is a laboratory frame of reference since the acoustic wavelength is much shorter than the size of the sample chamber. Therefore, particles move with different phases inside the narrow sound beam. The chamber as an entity remains immobile.

The question of the frame of reference is more complicated in the case of the electric field as a driving force (ESA). The wavelength of the electric field is much longer, and as a result all particles move in the same phase. This motion exerts a certain force on the chamber. The motion of the chamber depends on the mass of the chamber and mass of the sample. Depending on the construction of the instrument, the inertial system might be related to the chamber, to the center of mass, or to some intermediate case depending on the ratio of masses of the chamber and sample. It means that in the case of ESA the final expression relating measured ESA signal with properties of the dispersed system might contain a multiplier which depends on the mass of the chamber.

**Coupled Phase Model.** Let us consider the infinitesimal volume element in the dispersed system. There is a differential force acting on this element proportional to the pressure gradient of the sound wave  $\nabla P$ . This external force is applied to both the particles and liquid and is distributed between particles and liquid according to the volume fraction  $\varphi$ .

(15) Dukhin, A. S.; Goetz, P. J. *Acoustic Spectroscopy for Concentrated Polydisperse Colloids with High Density Contrast*. *Langmuir* **1996**, *12*, 4987-4997.

(16) Ahuja, A. S. Wave equation and propagation parameters for sound propagation in suspensions. *J. Appl. Phys.* **1973**, *44*, 4863-4868.

(17) Krut, H. R. *Colloid Science*; Elsevier: New York, 1952; Vol. 1: Irreversible Systems.

(18) Dukhin, S. S.; Derjaguin, B. V. *Electrokinetic Phenomena in Surface and Colloid Science*; Matijevic, E., Ed.; John Wiley & Sons: New York, 1974; Vol. 7.

(19) Shilov, V. N.; Zharkikh, N. I.; Borkovskaya, Yu. B. *Theory of Nonequilibrium Electrosurface Phenomena in Concentrated Disperse System. 1. Application of Nonequilibrium Thermodynamics to Cell Model*. *Colloid J.* **1981**, *43* (3), 434-438.

---

## AUTHOR INDEX ENTRIES

MSC: la990317g    BATCH: la8c10    VOLUME: 015    ISSUE: 018

Dukhin, A. S.

Shilov, V. N.

Ohshima, H.

Goetz, P. J.